High-density production of spin-polarized atomic hydrogen and deuterium

M. Poelker, K. P. Coulter,* R. J. Holt, C. E. Jones, R. S. Kowalczyk, L. Young, and B. Zeidman
Physics Division, Argonne National Laboratory, Argonne, Ilinois 60439-4843

D. K. Toporkov
Budker Institute for Nuclear Physics, 630 090 Novosibirsk, Russia
(Received 31 January 1994)

The electron polarization of hydrogen (H) and deuterium (D) atoms in a spin-exchange optical-pumping apparatus has been measured as a function of H (D) density and magnetic-field strength. The atomic density was varied between 4×10^{13} and 2.6×10^{14} atoms/cm^3 and the magnetic-field strength from 120 to 400 mT. The results suggest that the atoms approach spin-temperature equilibrium even though the magnetic fields are large compared to the critical fields of the atoms.

PACS number(s): 32.80.Bx, 29.25.Pj, 34.90.+q

I. INTRODUCTION

It has been proposed that spin-exchange optical pumping in a high magnetic field can yield polarized nuclei at high number densities without the need for actively performing radio frequency (rf) ground-state transitions [1]. Although high magnetic fields weaken the influence of the hyperfine coupling between the nucleus and the electron in a hydrogen atom, a high spin-exchange collision rate among hydrogen atoms is expected to increase the total probability for a hyperfine interaction to occur within a prescribed interaction period. In fact, it is believed that for sufficiently high hydrogen densities, atoms approach spin-temperature equilibrium.

Recent progress in the development of an intense, laser-driven source of spin-polarized H and D atoms [2] allows a test of the idea that at high densities, nuclei can become polarized despite a high magnetic field. To this end, we have measured the electron polarization of H and D atoms exiting a spin-exchange optical-pumping apparatus as a function of H (D) density and magnetic field strength. The H and D atoms provide an excellent test of this feature of the spin-exchange process since the large difference in the magnetic moments of the nuclei will give very different rates of approach to spin-temperature equilibrium.

In addition, spin-exchange optical pumping may prove useful for a variety of experiments in nuclear and particle physics. In particular, the use of dilute polarized gases as polarized nuclear targets in particle storage rings [3] allows for measurement of interesting spin-dependent phenomena, such as the spin structure of hadrons [4] and nuclear form factors [5]. Experiments with polarized nuclear targets have been performed and proposed at a number of storage ring facilities [6].

There is also strong interest in atomic physics for a dense, highly polarized gas of atoms. An electron-polarized hydrogen target is useful for experiments in atomic physics; for example, charge exchange in such a target can be used to form hydrogenlike heavy ions for study of parity violation [7]. Resonance experiments with polarized heavy ions to meausre hyperfine structure in few-electron systems can provide a stringent test of atomic structure calculations [8]. In addition, the target can be used for detailed studies of state-selective electron capture [9].

Spin-exchange optical pumping is a process whereby photon angular momentum is transferred to target nuclei through spin-exchange collisions with polarized, intermediate atoms (typically, alkali-metal atoms). The technique has long been known [10] and is reviewed in Ref. [11]. High electron polarization of H atoms has been demonstrated at low densities [12], however, earlier attempts at high densities met with limited success because of radiation trapping [13]. Recently, it was reported that high deuterium polarization could be obtained by spin-exchange optical pumping in a high magnetic field, thereby minimizing the effects of radiation trapping [2].

We report data for the spin-exchange optical-pumping process as a function of magnetic field and atomic density. The magnetic field strength ranged from 120 to 400 mT and the density was between 4×10^{13} and 2.6×10^{14} atoms/cm^3. Discrepancies between the experimental results and simple model predictions are discussed. Such discrepancies suggest that despite the high magnetic field, atoms within the spin-exchange cell evolve to spin-temperature equilibrium resulting in nuclear polarization.

II. THEORETICAL OVERVIEW

A simple model, in which only electronic spin states are considered, can be used to predict electron polarization values for H and D atoms within the spin-exchange optical-pumping apparatus. Such a model accounts for optical pumping of potassium atoms and spin-exchange collisions between potassium and H (D) atoms [14]. This model assumes that because hyperfine coupling in a high magnetic field is weak, nuclear spin can be ignored. Such

*Present address: Department of Physics, University of Michigan, Ann Arbor, Michigan 48109.

a system is represented in Fig. 1, which depicts optical pumping of potassium atoms in a high magnetic field with σ_+ laser light tuned to the D_1 transition. Potassium atoms in the $4\,^2S_{1/2}$, $m_e=-1/2$ ground state absorb the laser light and are excited to the $4\,^2P_{1/2}$ state. Atoms spontaneously decay to either of the two ground-state levels with a branching ratio of 2/3 to the $m_e=-\frac{1}{2}$ state and 1/3 to the $m_e=\frac{1}{2}$ state. After many optical-pumping cycles, the net result is that the $4\,^2S_{1/2}$, $m_e=\frac{1}{2}$ ground state becomes preferentially populated. Analogously, the $4\,^2S_{1/2}$, $m_e=-\frac{1}{2}$ state is preferentially populated when optical pumping is performed with σ_- laser light. Transitions between ground-state levels occur through spin-exchange collisions between potassium and H (D) atoms, a process indicated by the dashed line in Fig. 1. An expression for H (D) polarization can be deduced by considering the rate equations [14] that describe potassium and H (D) ground-state populations

$$P_{\mathrm{H\,(D)}}=\frac{\gamma_A}{\gamma_A+\gamma_{\mathrm{loss}}}P_{\mathrm{K}}\ , \tag{1}$$

where P_{K} is the potassium polarization, γ_A is the K-H(D) spin-exchange rate, and γ_{loss} is the H (D) polarization loss rate. The K-H(D) spin-exchange rate is given by $\gamma_A=n_{\mathrm{K}}\langle\sigma_{\mathrm{SE}}^{\mathrm{KH\,(D)}}v\rangle$, where n_{K} is the potassium density within the spin-exchange cell, $\sigma_{\mathrm{SE}}^{\mathrm{KH(D)}}$ is the K-H(D) spin-exchange cross section (7.4×10^{-15} cm^2) [15], and v is the thermally averaged relative K-H(D) velocity. The H (D) polarization loss rate is given by $\gamma_{\mathrm{loss}}=\Gamma_R+1/t_{\mathrm{dwell}}$, where Γ_R is the H (D) relxation rate including the effect of recombination and t_{dwell} is the characteristic time a H (D) atom remains in the spin-exchange cell. To arrive at this relatively straightforward expression for H (D) polarization, effects of nuclear spin and applied magnetic field were ignored.

A more sophisticated model has recently been proposed by Walker and Anderson [1] that considers effects of nuclear spin and applied magnetic field on polarized H (D) production in a spin-exchange optical-pumping apparatus. The model suggests that, although high magnetic fields generally weaken the influence of the hyperfine coupling between the nucleus and the electron, frequent H-H (D-D) collisions increase the total probability for a hyperfine interaction to occur. Under such a condition, atoms approach spin-temperature equilibrium and the nuclei become polarized through hyperfine interactions with polarized electrons.

To derive an expression for the time required for the hydrogen system to approach spin-temperature equilibrium, Walker and Anderson construct rate equations that describe the populations of the four magnetic substates of H (Fig. 2) in an arbitrary magnetic field under the influence of H-H spin-exchange collisions [1]. The population difference between states 2 and 4 is given by

$$P_2-P_4=(P_2-P_4)_0\exp(-t\sin^2\!2\theta/T_{\mathrm{H}})\ , \tag{2}$$

where the subscript 0 indicates initial condition and T_{H}^{-1} is the H-H spin-exchange rate given by $n_{\mathrm{H}}\langle\sigma_{\mathrm{SE}}^{\mathrm{HH}}v\rangle$, where n_{H} is the H density, $\sigma_{\mathrm{SE}}^{\mathrm{HH}}$ is the spin-exchange cross section (2×10^{-15} cm^2) [15], and $\langle v\rangle$ is the thermally averaged H-H velocity. The magnetic-field-dependent mixing angle θ is given by $\tan2\theta=\delta\nu_{\mathrm{hfs}}/g_s\mu_B B$, where $\delta\nu_{\mathrm{hfs}}$ is the ground-state hyperfine splitting in zero magnetic field and $g_s\mu_B B$ is the energy shift of the electron in a magnetic field B. In spin-temperature equilibrium, the population of a substate with magnetic quantum number m_f is given by $P_i=e^{\beta m_f}/N$, where $N=4\cosh^2(\beta/2)$ and β, referred to as the spin-temperature parameter [11], is defined in terms of the total angular momentum $\langle F_z\rangle=\tanh(\beta/2)$. For a hydrogen system in spin-temperature equilibrium, $P_2=P_4$ and from Eq. (2) the charactertistic time T_{ST} to approach spin-temperature equilibrium is given by

$$T_{\mathrm{ST}}=\frac{T_{\mathrm{H}}}{\sin^2\!2\theta}=\left[1+\left[\frac{g_S\mu_B B}{\delta\nu_{\mathrm{hfs}}}\right]^2\right]T_{\mathrm{H}}\ . \tag{3}$$

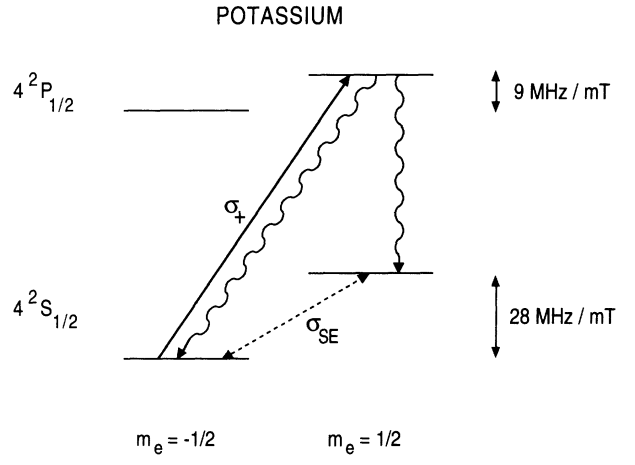

FIG. 1. Schematic diagram of a potassium atom in a high magnetic field. Optical pumping depletes the $m_e=-\frac{1}{2}$ ground-state sublevel for σ_+ light. Ground-state transitions occur via spin-exchange collisions with H or D atoms.

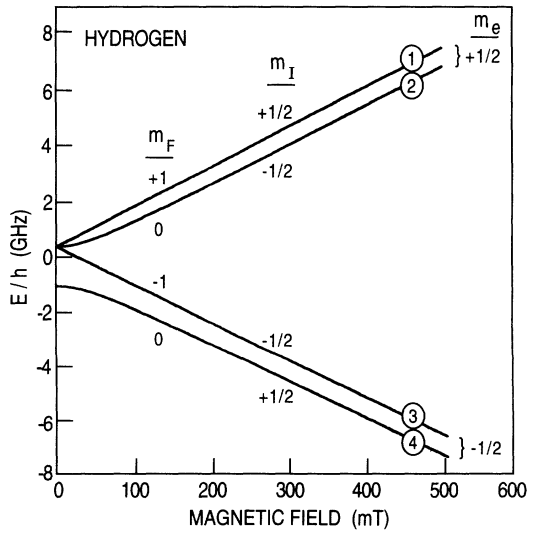

FIG. 2. Rabi diagram for H atoms in a magnetic field.

Equation (3) is approximatley true for deuterium as well.

To derive expressions for atomic and nuclear polarization for H atoms in a high magnetic field, Walker and Anderson construct rate equations that describe a hydrogen system under the influence of K-H and H-H spin-exchange collisions [1]

$$\frac{d\langle F_z\rangle}{dt}=\frac{1}{T_A}\left(\tfrac{1}{2}P_A-\langle F_z\rangle+\langle I_z\rangle\right), \tag{4}$$

$$\frac{d\langle I_z\rangle}{dt}=\frac{1}{2T_{\rm ST}}\left(\langle F_z\rangle-2\langle I_z\rangle\right), \tag{5}$$

where the following relations apply: $P_1+P_2+P_3+P_4=1$, $\langle F_z\rangle=P_1-P_3$, and $\langle I_z\rangle\approx(P_1-P_2-P_3+P_4)/2$. The quantity T_A is $1/\gamma_A$, as defined above. These differential equations can be solved for $\langle F_z\rangle$ and $\langle I_z\rangle$, the system total angular momentum and nuclear spin, respectively. To estimate the electron polarization of atoms leaving the spin-exchange cell, the system electron spin $\langle S_z\rangle$, given by $\langle S_z\rangle=\langle F_z\rangle-\langle I_z\rangle$, can be integrated over the appropriate Poisson distribution of dwell times to obtain

$$\langle\bar{S}_z\rangle=\left[\frac{A-D}{\Gamma+a}+\frac{B-E}{\Gamma+b}+\frac{(C-J)}{\Gamma}\right]\Gamma, \tag{6}$$

where $\Gamma=1/t_{\rm dwell}$ and the constants a,b,A,B,C,D,E,J are given in Table I. Equation (6) is also true for deuterium, but the coefficients a,b,A,B,C,D,E,J are different from those of hydrogen.

There are significant differences between the two models described above. In particular, the spin-exchange optical-pumping model, although appealing in its simplicity, does not distinguish between H and D atoms and does not consider effects associated with H (D) density and applied magnetic field. In contrast, the treatment of Walker and Anderson suggests that for comparable density and magnetic-field strength conditions, H atoms will approach spin-temperature equilibrium more quickly than D atoms because of the comparatively larger hyperfine splitting for H ($\delta\nu_{\rm hfs}^{\rm H}=1420$ MHz and $\delta\nu_{\rm hfs}^{\rm D}=327$ MHz). The difference in time that H and D atoms require to approach spin-temperature equilibrium can cause H and D electron polarization values to differ. Differences in polarization should be most apparent when $T_{\rm ST}$ values are made to vary about $t_{\rm dwell}$ with changing density and magnetic-field strength. Thus measurement of electron polarization for H and D atoms in an optical-pumping spin-exchange cell as a function atomic density and magnetic-field strength will provide an excellent test of these two models.

III. EXPERIMENTAL APPARATUS

In this experiment, molecular H (or D) is dissociated in a rf inductive discharge and sent into a spin-exchange cell containing potassium vapor (Fig. 3). The potassium atoms are optically pumped with laser light in the presence of a high magnetic field. Electron spin is transferred to H (D) atoms during collisions with polarized potassium atoms;

$$\mathrm{H}(\uparrow)+\mathrm{K}(\downarrow)\rightarrow\mathrm{H}(\downarrow)+\mathrm{K}(\uparrow). \tag{7}$$

H (D) atoms leave the spin-exchange cell and travel through a transport tube to a vacuum chamber that contains an atomic beam, electron-spin polarimeter.

A. Gas flow system and spin-exchange optical-pumping apparatus

Purified H (D) is obtained by electrolytically dissociating water and then diffusing H (D) through a thin palladium membrane. Beyond the palladium membrane, recombination occurs within stainless-steel tubing where H (D) is maintained at roughly 10 psi above atmospheric pressure. A needle valve (Granville-Philips series 216) is used to regulate the flow of H (D) to the spin-exchange optical-pumping apparatus. The exact flow rate is determined by measuring the pressure drop across a calibrated leak (MKS Model No. CFE-0.5).

The molecular H (D) then flows into a one-piece Pyrex glass apparatus that consists of three regions: a dissociator, a spin-exchange optical-pumping cell, and a transport tube. This one-piece construction ensures that no

TABLE I. The coefficients used in Eq. (6) to solve for the system's average electron spin $\langle\bar{S}_z\rangle$.

Coefficient	Hydrogen	Deuterium
A	$-\left[\dfrac{2\gamma_2 b+\gamma_1 a-4\gamma_1\gamma_2}{2\gamma_2 b+2\gamma_1 a-4\gamma_1\gamma_2}\right]P_A$	$-\left[\dfrac{\gamma_1 a+\frac{9}{4}\gamma_2 b-3\gamma_1\gamma_2}{2\gamma_1 a+\frac{3}{2}\gamma_2 b-2\gamma_1\gamma_2}\right]P_A$
B	$-(A+P_A)$	$-(A+\frac{3}{2}P_A)$
C	P_A	$\frac{3}{2}P_A$
D	$\dfrac{\gamma_2}{2\gamma_2-a}A$	$\dfrac{\gamma_2}{\frac{3}{2}\gamma_2-a}A$
E	$-(D+P_A/2)$	$-(D+P_A)$
J	$P_A/2$	P_A
a	$\gamma_1+\gamma_2-\sqrt{(\gamma_1)^2+(\gamma_2)^2}$	$\frac{1}{4}(3\gamma_2+4\gamma_1-\sqrt{9\gamma_2^2+16\gamma_1^2+8\gamma_1\gamma_2})$
b	$\gamma_1+\gamma_2+\sqrt{(\gamma_1)^2+(\gamma_2)^2}$	$\frac{1}{4}(3\gamma_2+4\gamma_1+\sqrt{9\gamma_2^2+16\gamma_1^2+8\gamma_1\gamma_2})$
γ_1	$\frac{1}{2}\gamma_A$	$\frac{1}{2}\gamma_A$
γ_2	$\frac{1}{2}\gamma_{ST}$	$\frac{1}{2}\gamma_{ST}$

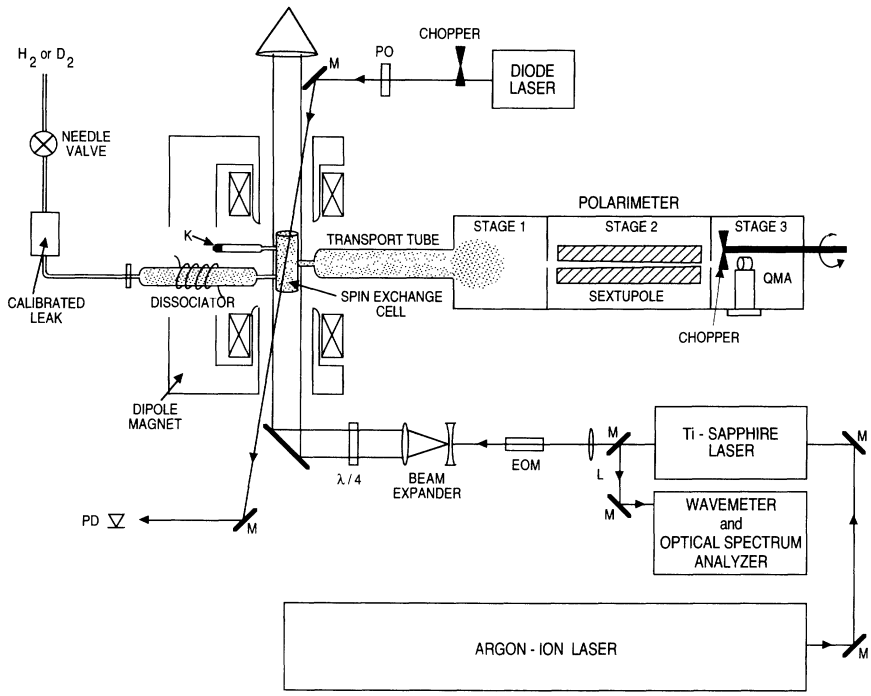

FIG. 3. Schematic diagram of the spin-exchange optical-pumping apparatus. *M*, mirror; *L*, lens; EOM, electro-optic modulator; $\lambda/4$, quarter-wave plate; PD, photodiode; PO, polarizing optic (quarter-wave plate or depolarizer); QMA, quadrupole mass analyzer.

air leaks exist near the rf discharge, circumvents the need for vacuum seals between regions, and also minimizes unwanted surface area between regions to reduce the likelihood of recombination.

Molecular H (D) is dissociated in a rf inductive discharge created by a 13-turn coil 3.5 cm in diameter, which is part of an *LC* tuned circuit. The coil is suspended around the dissociator region and rests within a grounded brass cylinder. Grounding straps are also placed above and below the cylinder to ensure confinement of the discharge to the dissociator region. The *LC* circuit resonates at approximately 50 MHz and dissociation performance is optimized when approximately 30 W of rf power is absorbed by the hydrogen.

Upon dissociation, atomic H (D) flows continuously through a small aperture (0.9 mm diameter) into a cylindrical cell (referred to as the spin-exchange cell) that also contains potassium vapor. Potassium atoms enter the spin-exchange cell through a separate aperture (0.9 mm diameter) from a heated sidearm that contains approximately 1 g of potassium metal. The spin-exchange cell is positioned between the pole tips of a dipole magnet with the long axis of the cell oriented parallel to the magnetic field. The potassium vapor is optically pumped with circularly polarized laser light that propagates along the direction of the magnetic field. The H (D) atoms become polarized through repeated spin-exchange collisions with the polarized potassium atoms.

Polarized H (D) and potassium atoms exit the spin-exchange cell through an opening that leads to a region of low magnetic field, referred to as the transport tube (250 mm long, 19 mm diameter). The transport tube guides the atoms toward an atomic beam, electron-spin polarimeter (described below) and also provides a region where rf ground-state transitions can be induced.

The spin-exchange cell and the transport tube must be heated to $\sim 250\,^{\circ}\mathrm{C}$ in order to prevent potassium from condensing on the walls. To achieve this end, the spin-exchange cell and transport tube rest within a glass sleeve. Hot air is forced between the sleeve and the outer surface of the spin-exchange cell and the transport tube. The walls of the spin-exchange cell and the transport tube are coated with "drifilm" to prevent recombination and depolarization of H,D and potassium atoms at the walls. Drifilm, in contrast to paraflint, can withstand the high cell temperature necessitated by the use of potassium vapor. The coating process is described in Ref. [16].

The dimensions of the spin-exchange cell and the diameter of the hole leading to the transport tube were chosen by requiring that (i) the characteristic time an atom spends in the spin-exchange cell be long enough to ensure a high density of H (D) atoms within the spin-exchange cell and (ii) atom-wall collisions are minimized to prevent depolarization and molecular recombination. A cylindrical spin-exchange cell (45 mm long$\times$22 mm wide) was chosen for this experiment. The exit hole was chosen to be 3.1 mm in diameter. Such a cell geometry allows for efficient optical pumping and provides an adequate compromise between the competing requirements listed above. The characteristic time for H (D) atoms within the spin-exchange cell was calculated to be 4.1 msec (5.8 msec) as given by $t_{\mathrm{dwell}}=4V/vAK$, where V is the spin-exchange cell volume, v is the thermally averaged velocity, A is the area of the exit hole, and K is the Knudsen factor. An atom experiences approximately 700 wall collisions in the spin-exchange cell before entering the transport tube ($N_w=\delta/AK$, where δ is the surface area of the spin-exchange cell). Such a number is considerably less than that found to produce recombination on drifilm-coated Pyrex [17]. With these dimensions, operating H and D densities in the spin-exchange cell were between 4×10^{13} and 2.6×10^{14} atoms/cm^3.

B. Polarimeter and vacuum system

Polarized H (D) atoms travel through the transport tube toward a vacuum chamber that contains an atomic beam, electron-spin polarimeter. The polarimeter consists of a permanent sextupole magnet and a quadrupole mass analyzer (QMA). The sextupole magnet focuses electron "spin-up" atoms and defocuses electron "spin-down" atoms where the terms "up" and "down" refer to the electron-spin orientation relative to the local magnetic field of the sextupole magnet. Atoms and molecules that travel through the sextupole magnet are detected with the QMA that is positioned at the focus of the magnet. A Monte Carlo simulation indicates that a majority ($\sim 90\%$) of the atoms that are detected by the polarimeter scatter from the walls of the transport tube. Electron polarization is evaluated by comparing QMA signals when the laser beam is incident upon the spin-exchange cell and then blocked,

$$P_e = \frac{N_{\sigma\pm}}{N_0} - 1 \ , \tag{8}$$

where N_0 refers to the QMA signal when the laser beam is blocked (1 amu detection for H and 2 amu detection for D), $N_{\sigma\pm}$ is the QMA signal when the laser beam is incident upon the spin-exchange cell, and $\sigma\pm$ refers to the circular polarization of the laser light.

The QMA is also used to determine degree of dissociation by comparing molecular throughput with and without a discharge in the dissociator ($M_{\rm on}$ and $M_{\rm off}$, respectively)

$$D_{\rm dis} = 1 - \frac{M_{\rm on}}{M_{\rm off}} \ . \tag{9}$$

A chopper, located downstream from the sextupole magnet, modulates the H (D) flow to the QMA. The ambient H (D) background is suppressed using a lock-in amplifier to measure only the chopped signal from the QMA. Dissociator performance is shown in Fig. 4, which depicts the percentage of total deuterium density that exists in the spin-exchange cell in atomic form. Although the data in Fig. 4 represent "best-ever" performance, degree of dissociation values $\approx 75\%$ are regularly obtained under normal operating conditions. Knowledge of degree of dissociation allows calculation of the atomic density within the spin-exchange cell, from

$$n_{\rm eff} = \frac{4L}{vAK} D_{\rm dis} = n D_{\rm dis} \ , \tag{10}$$

where L is the flow rate of H (D) atoms through the apparatus, A is the area of the exit hole in the spin-exchange cell, and n is the total H (D) density in both atomic and molecular form.

The electron-spin, atomic beam polarimeter rests within a vacuum system composed of three differentially pumped regions to minimize H (D) background pressure at the QMA. The majority of H (D) is pumped from the system in the first region with a turbomolecular pump and a titanium-sublimation pump. The first region pressure is typically 10^{-6} Torr under standard operating conditions. Pressure is reduced by a factor of 10 in the second region, where the permanent sextupole magnet is located, by a second titanium-sublimation pump. In the final region, where the QMA is located, an ion pump is used to reduce the pressure by another order of magnitude.

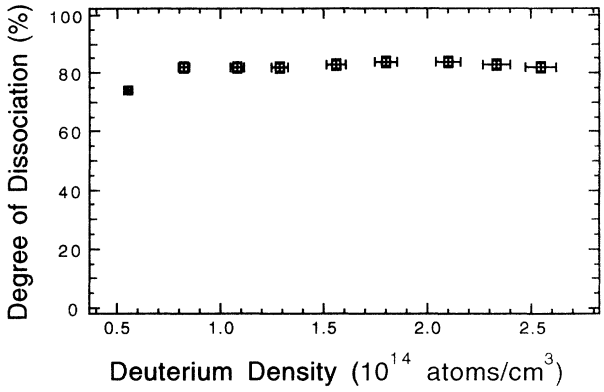

FIG. 4. Degree of dissocation vs total deuterium density within the spin-exchange cell.

C. Pump laser and optics

A tunable, single-frequency titanium-sapphire laser (Coherent 899-01) is used to optically pump the potassium vapor. Three intracavity elements (birefringent tuning filter, thick étalon, and thin étalon) allow precise laser-frequency tuning to the potassium D_1 line ($\lambda_{4^2S_{1/2}\rightarrow 4^2P_{1/2}} = 770.1$ nm). A small portion of the laser output is sent to an optical spectrum analyzer (Fabry-Pérot étalon) and wavemeter to monitor laser-frequency stability and wavelength. The majority of the laser output is focused into an electro-optic modulator (EOM) driven with 20 W of amplified white noise. The EOM serves to broaden the laser linewidth from 10 MHz to approximately 1 GHz. With this technique [18], the laser linewidth closely matches the width of the Doppler-broadened D_1 line and ensures that both hyperfine sublevels of the $4^2S_{1/2}$ ground state are optically pumped. The laser beam is then expanded, collimated, and passed through a quarter-wave plate. Circularly polarized light is directed along the central axis of the dipole magnet and into the spin-exchange cell where potassium vapor is spin polarized through optical pumping. The dipole magnet field strength in the region of the spin-exchange cell is uniform to within 3% and is greater than 100 mT to minimize radiation trapping and maximize potassium polarization [19]. Typically, 3 W of laser power are incident upon the spin-exchange cell. When the quarter-wave plate is oriented to induce $\Delta m = +1$ transitions, the potassium vapor is polarized electron spin up with respect to the magnetic field. When the quarter-wave plate is rotated 90°, $\Delta m = -1$ transitions are induced and the potassium vapor is polarized electron spin down. In a high magnetic field, switching between electron spin-up and electron spin-down polarized H (D) also requires a slight change in laser frequency which is accomplished by tilting the thick and thin étalons.

D. Probe laser: Potassium density and polarization measurements

Potassium density and polarization within the spin-exchange cell are measured throughout the duration of the experiment to ensure that any change in H (D) polarization is not merely due to a change in alkali-metal conditions. Measurements are made with a tunable, single-frequency probe laser and rely on probe laser transmission through the spin-exchange cell

$$I(\nu)=I_0 e^{-\sigma(\nu)n_K l}, \tag{11}$$

where $I(\nu)$ is the probe laser intenstiy, I_0 is the probe laser intensity when the laser frequency is tuned far from resonance, $\sigma(\nu)$ is the absorption cross section, n_K is the potassium density, and l is the spin-exchange cell length. Rewriting Eq. (11) and integrating over frequency yields

$$\int \ln\frac{I_0}{I(\nu)}d\nu = n_K l \int \sigma(\nu)d\nu . \tag{12}$$

The term $\int\sigma(\nu)d\nu$ is equal to $\pi c r_e f$, where $r_e=e^2/mc^2$ and f is the oscillator strength of the transition. Measurement of the quantity $I(\nu)$ as the probe-laser frequency is scanned across the D_1 line allows determination of the potassium density. Potassium polarization is determined by calculating the ratio of two $\int\ln[I_0/I(\nu)]d\nu$ values, when the pump laser is incident upon the spin-exchange cell and when blocked. It should be noted that at typical operating temperatures, the probe-laser beam is completely absorbed over a range of frequencies near line center. Under such a circumstance, a Gaussian curve is fit to the wings of the absorption profile and the area under the fitted curve is used in calculating density or polarization.

Potassium density and polarization measurements are made with a single-mode diode laser (SHARP model LT024). No optical feedback is necessary to tune the laser frequency across the D_1 line. The diode-laser linewidth is approximately 20 MHz, which is considerably less than the Doppler-broadened linewidth of potassium at typical operating temperatures. The linearly polarized probe-laser output is directed through polarizing optics and then into the spin-exchange cell nearly collinear but counterpropagating to the pump-laser beam. The probe-laser frequency is varied by ramping the diode-laser drive current [20] and a photodiode is used to measure the change in probe-laser transmission through the spin-exchange cell. The constant increase in probe-laser power that results from ramping the diode-laser drive current is divided from the photodiode trace using the signal from another photodiode that monitors a portion of the probe-laser beam that does not travel through the spin-exchange cell.

Examples of probe-laser transmission through the spin-exchange cell versus probe-laser frequency are shown in Figs. 5(b)–5(e) for various experimental conditions and illustrate the technique used to determine potassium density and polarization. Probe-laser frequency calibration is obtained by monitoring probe-laser transmission through a Fabry-Pérot étalon with a free spectral range of 7.5 GHz [Fig. 5(a)]. In all cases depicted in Fig. 5, the deuterium density within the spin-exchange cell was $\approx 7\times10^{13}$ atoms/cm^3 and the temperature of the potassium reservoir was 180 °C. To obtain the trace in Fig. 5(b), the probe-laser beam was directed through a depolarizer and then into the spin-exchange cell with the pump-laser beam blocked. No magnetic field was applied to the spin-exchange cell for this purpose. The weak probe-laser beam (25 μW) is completely absorbed over a range of frequencies near line center. Calculation of $\int\ln[I_0/I(\nu)]d\nu$ indicates that potassium density within the spin-exchange cell is 2×10^{11} atoms/cm^3. For Fig. 5(c), the probe-laser beam was directed into the spin-exchange cell after passing through a quarter-wave plate oriented to excite $\Delta m=-1$ transitions. The magnetic field was set to 400 mT. The applied magnetic field shifts the magnetic substates; maximum probe-laser absorption is observed to occur at a different probe-laser frequency from that observed in Fig. 5(b). In Fig. 5(d), both the probe- and the pump-laser beams were directed into the spin-exchange cell with laser frequency and polarization chosen to excite $\Delta m=-1$ transitions. No attempt was made to tailor the pump-laser linewidth to that of the Doppler-broadened line (i.e., no EOM was used). Significant probe-beam absorption implies the po-

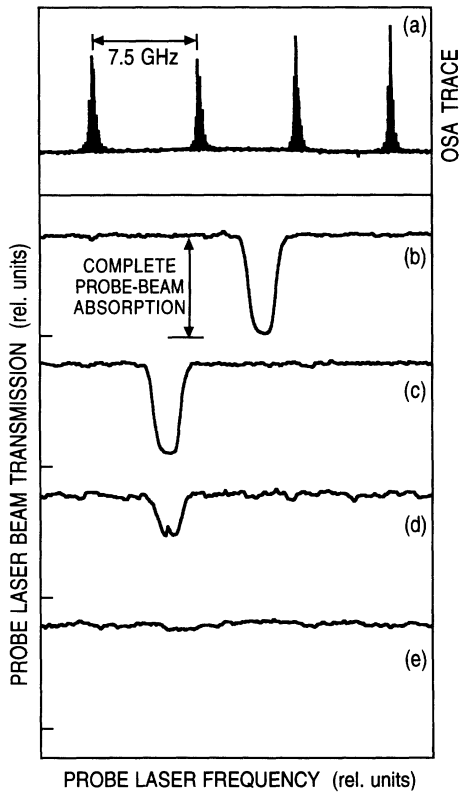

FIG. 5. Probe-laser transmission through the spin-exchange cell as a function of probe-laser frequency: (a) probe-laser transmission through Fabry-Pérot étalon used for frequency calibration; (b) $B=0$, pump laser blocked; (c) $B=4$ kG, pump laser blocked; (d) $B=4$ kG, narrow-band pump laser directed into the spin-exchange cell; (e) $B=4$ kG, frequency-broadened pump laser directed into the spin-exchange cell.

tassium is poorly polarized ($P_K \approx 30\%$). Decreased absorption near the center of the absorption profile is an indication that the narrow-band pump laser (≈ 10 MHz linewidth) is exciting relatively few potassium atoms (i.e., only those that have trajectories nearly orthogonal to the pump-laser beam direction). In Fig. 5(e), the pump-laser beam was directed through the EOM; very little of the probe-laser beam is absorbed when the probe-laser frequency is scanned across the line. The trace clearly indicates that efficient optical pumping occurs when the laser linewidth is broadened using the EOM technique. Potassium polarization is calcualted to be 95% using the probe-laser transmission traces in Figs. 5(c) and 5(e).

IV. EXPERIMENTAL RESULTS

The electron polarization of H and D atoms emitted from the spin-exchange optical-pumping apparatus was measured using the atomic beam, electron-spin polarimeter. In Fig. 6(a), polarization values are plotted versus atomic density within the spin-exchange cell. Measurements were made over a range of dissociator region pressures where degree of dissocation was high and nearly constant ($\approx 75\%$). The potassium-reservoir temperature was maintained at 188 °C, resulting in a potassium density within the spin-exchange cell of approximately 4×10^{11} atoms/cm^3. Approximately 3 W of pump-laser power were incident upon the spin-exchange cell. The data were obtained with a magnetic field of 400 mT in the region of the spin-exchange cell. Polarization values are high ($\approx 70\%$) for H and D atoms at lower densities. At higher densities, polarization values decrease, although D polarization drops more severely than H polarization. Potassium polarization was also measured throughout the experiment and values are shown plotted versus H (D) atomic density in Fig. 6(b). Potassium polarization is observed to decrease with increasing H (D) density, although values remain high ($\approx 90\%$) over the entire range of densities tested. Repeated measurements of polarization made over a period of several minutes with operating conditions unchanged indicate that H and D polarization can be measured to within a standard deviation of 2% and potassium polarization to within 5%.

The electron polarization of H and D atoms emitted from the spin-exchange optical-pumping apparatus was also measured for three different magnetic fields (120, 220, and 400 mT) in the spin-exchange cell as shown in Fig. 7. Molecular dissociation, pump-laser power, and potassium-density conditions were similar to those described above. The data were acquired by holding the

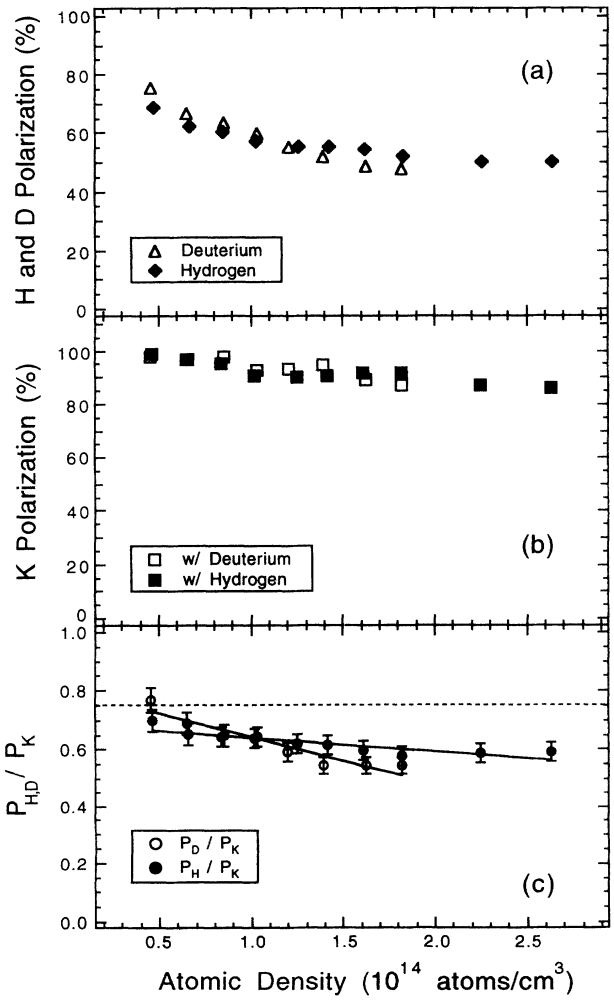

FIG. 6. Polarization values vs atomic density within the spin-exchange cell: (a) H and D polarization, (b) potassium polarization, and (c) ratios P_H/P_K and P_D/P_K. The dashed line in (c) is a simple model estimate of $P_{H,D}/P_K$.

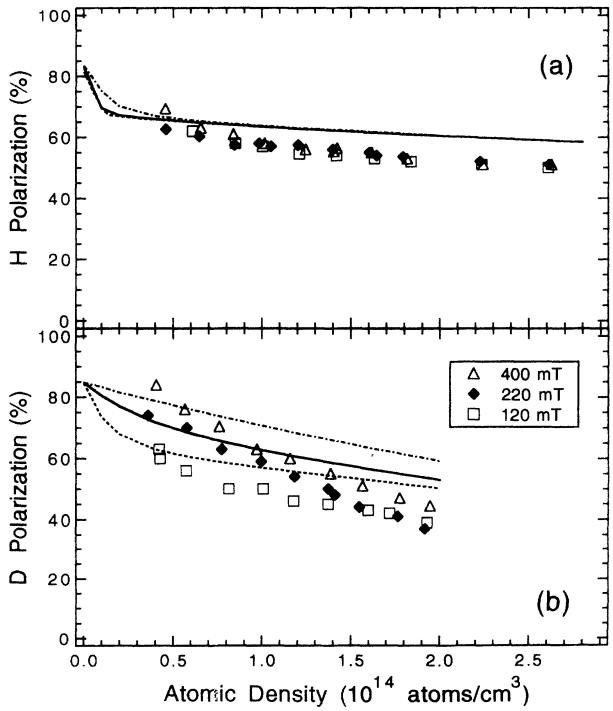

FIG. 7. Polarization values vs atomic density and magnetic field: (a) hydrogen and (b) deuterium. The smooth lines are theoretical predictions obtained using Eq. (6) and the model of Walker and Anderson; 400 mT (dot-dashed line), 220 mT (solid line), and 120 mT (dashed line).

magnetic field constant and varying the atomic density. The magnetic field was then changed and a new set of data were obtained over a similar range of atomic densities. The magnetic-field dependence of the data clearly demonstrates different behavior for H and D atoms. Values of H polarization are relatively insensitive to changing magnetic field [Fig. 7(a)], whereas D polarization values depend significantly upon magnetic field [Fig. 7(b)].

V. DISCUSSION

The shortcomings of the simple spin-exchange optical-pumping model are evident when attempting to explain the atomic density and magntic-field dependence of the H and D polarization data in Figs. 6 and 7. The simple model suggests that the ratio of H or D polarization to potassium polarization ($P_{H,D}/P_K$) should remain constant as a function of H (D) density because the quantity $\gamma_A/(\gamma_A+\gamma_{loss})$ in Eq. (1) is independent of this variable. Under operating conditions described above, the K-H(D) spin-exchange rate is approximately 760 sec^{-1}. The polarization loss rate is estimated to be roughly 250 sec^{-1} [21]. Then according to Eq. (1), the ratio $P_{H,D}/P_K$ is equal to 0.75. Measured values of $P_{H,D}/P_K$, as well as the estimated value, are plotted versus atomic density within the spin-exchange cell in Fig. 6(c). Clearly, the measured ratio varies with changing density, in contradition to the simple-model prediction and furthermore, the ratio differs for H and D atoms. A straight-line fit to the data reveals that as density increases, the ratio P_H/P_K decreases at a rate of $(-4.6\pm0.9)\times10^{-16}$ $(atoms/cm^3)^{-1}$. The ratio P_D/P_K decreases more severely at a rate of $(-16.0\pm2.3)\times10^{-16}$ $(atoms/cm^3)^{-1}$. The simple model cannot account for the different behavior between H and D atoms. The simple model also fails to account for the variation in D polarization values observed with changing magnetic field visible in Fig. 7(b). The inability of the simple model to predict H and D polarization behavior with changing density and field suggests that the model inadequately describes the process of spin-exchange optical pumping in dense samples of H and D.

The density and the magnetic-field dependence of H and D polarization data, however, are consistent with the treatment of Walker and Anderson. Their model predicts that the large difference in the magnetic moments of the nuclei will give very different rates for approach to spin-temperature equilibrium. For comparable densities, H atoms will approach spin-temperature equilibrium more quickly than D atoms because of the larger hyperfine splitting for H ($\delta\nu_{hfs}^H=1420$ MHz and $\delta\nu_{hfs}^D=327$ MHz). Atoms approach spin-temperature equilibrium when $T_{ST}<t_{dwell}$. For H atoms in the spin-exchange cell, T_{ST} values are less than t_{dwell} over the entire range of densities and fields tested ($0.03<T_{ST}<3.0$ msec and $t_{dwell}^H=4.1$ msec). Because H atoms quickly approach spin-temperature equilibrium within the spin-exchange cell, H polarization is observed to be relatively insensitive to the changing density and magnetic field. For D atoms, however, T_{ST} values span a range about t_{dwell} ($0.43<T_{ST}<67$ msec and $t_{dwell}^D-5.8$ msec). Deuterium atoms approach spin-temperature equilibrium within the spin-exchange cell only for high density and low field conditions. As a result, D polarization is observed to be more sensitive to changing density and magnetic field.

The model of Walker and Anderson was used to make theoretical predictions of electron polarization for H and D atoms within the spin-exchange cell. Theoretical electron polarization values obtained using Eq. (6) are plotted as a function of atomic density in Fig. 7. These predictions were obtained using measured values of potassium density and polarization. Only H-H (D-D) spin-exchange collisions within the spin-exchange cell were considered. The effects of collisions within the transport tube and polarization loss due to wall relaxation were ignored. The theoretical predictions of H and D polarization as a function of atomic density and magnetic field display similar behavior to that of the data [22]. For H atoms, theoretical and measured values of polarization are insensitive to changing magentic field, whereas for D atoms, theoretical and measured values of polarization vary significantly with changing magnetic field. Theoretical polarization values, however, tend to overestimate H and D polarization, especially at higher atomic densities. Better quantitative agreement between theory and experiment may result if polarization loss due to wall relaxation were accounted for in the model.

VI. CONCLUSION

The density and field dependence of the H and D polarization data suggest that H and D atoms approach spin-temperature equilibrium within the spin-exchange optical pumping. This is the best evidence that the spin-exchange model of Walker and Anderson is correct. This implies that at high atomic densities nuclei become polarized even at fields that are much higher than the critical field because of the high frequency of spin-exchange collisions. Efforts [23] to measure nuclear polarization directly for relatively dense polarized deuterium samples are in progress.

ACKNOWLEDGMENTS

We thank Joe Gregar for his expert glass blowing of the optical-pumping spin-exchange apparatus. We also thank Erhard Steffens for the loan of the permanent sextupole magnet. Valuable assistance was offered throughout the experiment from students Germaline Calagday, Taliver Heath, Jamie Kustak, and David Flory. This work was supported by the U.S. Department of Energy, Nuclear Physics Division and the Office of Basic Sciences, under Contract No. W-31-109-ENG-38.

[1] T. Walker and L. W. Anderson, Nucl. Instrum. Methods Phys. Res., Sect. A **334**, 313 (1993); T. Walker and L. W. Anderson, Phys. Rev. Lett. **71**, 2346 (1993).

[2] K. P. Coulter *et al.*, Phys. Rev. Lett. **68**, 174 (1992); M. Poelker *et al.*, in *Workshop on Polarized Ion Sources and Polarized Gas Targets, University of Wisconsin, Madison, WI, 1993,* edited by L. W. Anderson and W. Haberli, AIP Conf. Proc. No. 293 (AIP, New York, 1994), p. 125.

[3] G. I. Budker, A. P. Onuchin, S. G. Popov, and G. M. Tumajkin, Yad. Fiz. **6**, 775 (1967); R. J. Holt, in *Proceedings of the Conference on Intersections Between Particle and Nuclear Physics,* AIP Conf. Proc. No. 123, edited by Richard E. Mische (AIP, New York, 1984), p. 499; R. J. Holt, in Proceedings of the Workshop on Polarized Targets in Storage Rings, ANL Report No. 84-50, 1984 (unpublished), p. 103.

[4] M. W. Alguard *et al.*, Phys. Rev. Lett. **37**, 1258 (1976).

[5] R. J. Holt, M. C. Green, L. Young, R. S. Kowalczyk, D. F. Geesaman, B. Zeidman, L. S. Goodman, and J. Napolitano, Nucl. Phys. A **446**, 389c (1985).

[6] Experiments have been performed and proposed that use internal polarized targets at the VEPP-3 ring in Novosibirsk [R. Gilman *et al.*, Phys. Rev. Lett. **65**, 1733 (1990)], the UNK ring at Serpukov [D. G. Crabb *et al.*, *ibid.* **65**, 3241 (1990)], the HERA ring at DESY [HERMES collaboration, Report No. DESY-PRC-90-01, 1990 (unpublished)], the cooler ring at IUCF [J. Sowinski and J. van den Brand, Indiana University Cyclotron Facility Proposal No. CE-25, 1990 (unpublished); K. Pitts, Indiana University Cyclotron Facility Proposal No. CE-26, 1990 (unpublished)], and the stretcher rings at MIT-Bates [R. Milner *et al.*, MIT-Bates Proposal No. 89-12, 1989 (unpublished)], NIKHEF, and Saskatoon.

[7] R. W. Dunford and R. R. Lewis, Phys. Rev. A **23**, 10 (1981).

[8] S. N. Panigraphy, R. W. Dougherty, T. P. Das, and J. Andriessen, Phys. Rev. A **40**, 1765 (1989); C. J. Liu *et al.*, Phys. Rev. Lett. **64**, 1354 (1990); S. Garpman, I. Lindgren, J. Lindgren, and J. Morrison, Z. Phys. A **276**, 167 (1976).

[9] R. K. Janev and H. Winter, Phys. Rep. **117**, 265 (1985).

[10] H. G. Dehmelt, Phys. Rev. **109**, 381 (1958).

[11] W. Happer, Rev. Mod. Phys. **44**, 169 (1972).

[12] S. G. Redsun, R. J. Knize, G. D. Cates, and W. Happer, Phys. Rev. A **42**, 1293 (1990).

[13] L. Young *et al.*, Nucl. Phys. A **497**, 529c (1989).

[14] T. E. Chupp *et al.*, Phys. Rev. C **36**, 2244 (1987).

[15] H. R. Cole and R. E. Olson, Phys. Rev. A **31**, 2137 (1985).

[16] D. R. Swenson and L. W. Anderson, Nucl. Instrum. Methods Phys. Res., Sect. B **29**, 627 (1988).

[17] A. Maudl and A. Salop, J. Appl. Phys. **44**, 4776 (1973).

[18] D. S. Elliott and S. J. Smith, J. Opt. Soc. Am. B **5**, 1927 (1988).

[19] D. Tupa, L. W. Anderson, D. L. Huber, and J. E. Lawler, Phys. Rev. A **33**, 1045 (1986); D. Tupa and L. W. Anderson, *ibid.* **36**, 2142 (1987); L. W. Anderson and Thad Walker, Nucl. Instrum. Methods Phys. Res., Sect. A **316**, 123 (1992).

[20] C. E. Wieman and L. Hollberg, Rev. Sci. Instrum. **62**, 1 (1991).

[21] L. Young, R. J. Holt, M. C. Green, and R. S. Kowalczyk, Nucl. Instrum. Methods Phys. Res., Sect. B **24**, 963 (1987). (This reference describes measurements of polarization loss rates for potassium on "drifilm"-coated copper. A polarization loss rate of 710–1000 sec^{-1} is measured. It is reasonable to assume that H and D polarization loss rates will be smaller. Drifilm is described in Ref. [16].)

[22] To obtain the theoretical plots in Fig. 7, a H-H (D-D) spin-exchange cross section equal to 8×10^{-15} cm^2 was used. This value is approximately four times larger than that in Ref. [15].

[23] C. E. Jones *et al.*, in *Workshop on Polarized Ion Sources and Polarized Gas Targets, University of Wisconsin, Madison, WI, 1993* (Ref. [2]), p. 131.

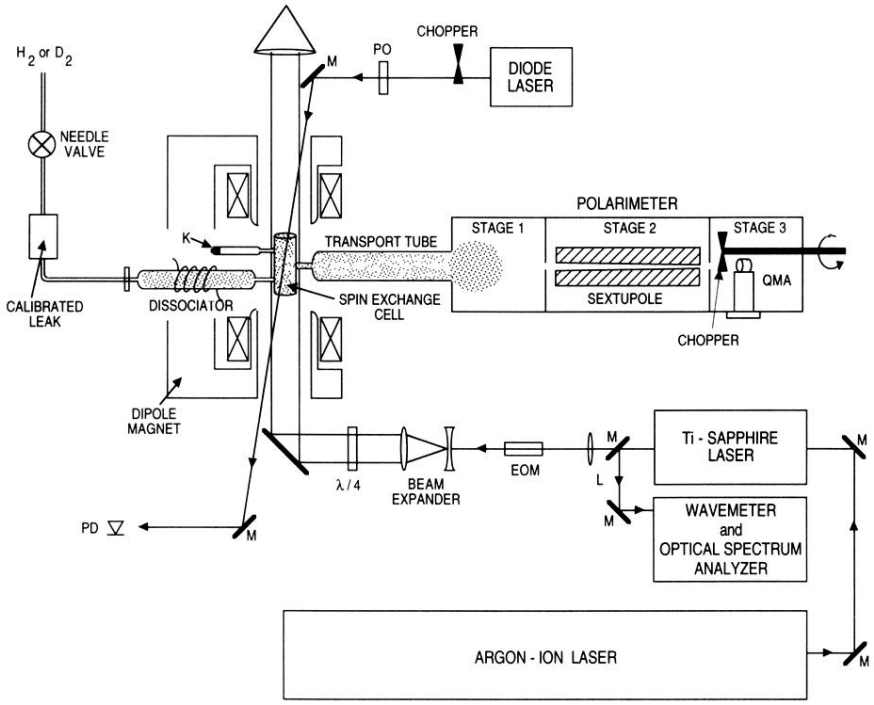

FIG. 3. Schematic diagram of the spin-exchange optical-pumping apparatus. *M*, mirror; *L*, lens; EOM, electro-optic modulator; $\lambda/4$, quarter-wave plate; PD, photodiode; PO, polarizing optic (quarter-wave plate or depolarizer); QMA, quadrupole mass analyzer.